DesignCon 2019

A Fast and Simple RFI Mitigation Method without Compromising Signal Integrity

Qiaolei Huang, Missouri University of Science and Technology
[qh5x4@mst.edu]

Ling Zhang, Missouri University of Science and Technology
[lzd76 @mst.edu]

Yang Zhong, Missouri University of Science and Technology
[zhongya@mst.edu]

Jagan Rajagopalan, Amazon Lab126
[rrajagop@amazon.com]

Deepak Pai, Amazon Lab126
[hosadurg@amazon.com]

Chen Chen, Amazon Lab126
[cchc@amazon.com]

Amit Gaikwad, Amazon Lab126
[gaikwada@amazon.com]

Chulsoon Hwang, Missouri University of Science and Technology
[hwangc@mst.edu]

Jun Fan, Missouri University of Science and Technology
[jfan@mst.edu]

Abstract

In modern wireless consumer electronic devices, there is an increasing need for smaller, compact, and denser design. This often requires wireless components like transceiver, front-end and antenna to be placed very close to noise sources like memory, power supply, and main processor in the device. Electromagnetic noise from noise sources interferes with wireless receiver components causing radio frequency interference (RFI) issues in the device. As a result, wireless performance metrics like range and throughput is degraded, which impacts the user experience. In this paper, a popular consumer electronic device is studied. The device has many complex subsystems like CPU, DDR memory, and power supply co-located with Wi-Fi circuitry. Due to small size, the device has RFI issues from CPU memory interface, which affects the Wi-Fi range. Typically, RFI problem can be mitigated from a mechanical design perspective by adding shield can, or from a signal integrity perspective by modifying clock and slew rate of the high-speed signals. In this paper, a novel RFI mitigation method is proposed. Through near-field scanning, an equivalent dipole moment of the noise source (CPU and DDR3) is reconstructed, and the near-field components of the victim (Wi-Fi antenna) are measured. By determining relationship between dipole moment and antenna near field, the noise source is rotated by a certain angle to reduce RFI. Rotating the source to reduce RFI is implemented in such a way that it doesn't compromise signal integrity, and it doesn't require an additional shield can. New boards with the suggested changes are fabricated and the measured results show a good RFI reduction (up to 8 dB) compared to original boards.

Author(s) Biography

Qiaolei Huang received the B.E. degree in Electrical and Computer Engineering from Huazhong University of Science and Technology, Wuhan, China, in 2013, and the M.S. degree in electrical engineering from EMC Laboratory, Missouri University of Science and Technology, Rolla, MO, USA, in 2016. He is currently working toward the Ph.D. degree in electrical engineering at EMC Laboratory, Missouri University of Science and Technology, Rolla, MO, USA. His research interests include radio frequency interference, radiated emission modeling, and EMC measurement method.

Ling Zhang received the B.S. degree in electrical engineering from Huazhong University of Science and Technology, Wuhan, China in June 2015, and MS degree from Missouri S&T in Dec 2017. He worked in Cisco as a student intern from Aug 2016 to Aug 2017. He is now pursuing his PhD degree in EMC lab, Missouri S&T. His research interests include machine learning applications in PI/SI/EMC, RFI source reconstruction and coupling paths analysis, and Emission Source Microscopy (ESM) technique for EMI source localization.

Yang Zhong received the B.S. degree in Optoelectronics Science and Engineering from Huazhong University of Science and Technology, Wuhan, China, in 2017. He is currently a MS student in electrical engineering at EMC Laboratory, Missouri University of Science and Technology, Rolla, MO, USA. His research interest is electromagnetic interference.

Jagan Rajagopalan is a Senior RF System Engineer in Wireless Technology Group of Amazon Lab126.

Deepak Pai is an RF System Engineer in Wireless Technology Group of Amazon Lab126.

Chen Chen is an RF System manager in Wireless Technology Group of Amazon Lab126.

Amit Gaikwad is a Senior RF System manager in Wireless Technology Group of Amazon Lab126.

Chulsoon Hwang is with EMC laboratory at Missouri S&T (Formerly University of Missouri−Rolla) as an assistant professor. He received his PhD degree at KAIST in 2012 and worked at Samsung Electronics as a senior engineer from 2012 to 2015. He has authored or co-authored 50+ IEEE journal/conference papers and received a best paper award at AP-EMC 2017, DesignCon 2018 and an outstanding young scientist award at AP-EMC 2018. His research area includes RF desense, signal/power integrity, and electromagnetic interference.

Jun Fan is currently the Director of the Industry-University Cooperative Research Center (IUCRC) for EMC, supported by the National Science Foundation (NSF) and led by the Missouri S&T EMC Laboratory where he is also the Director.
Dr. Fan received his B.S. and M.S. degrees in Electrical Engineering from Tsinghua University, Beijing, China, in 1994 and 1997, respectively. He received his Ph.D. degree in Electrical Engineering from the University of Missouri-Rolla in 2000. From 2000 to 2007, he worked for NCR Corporation, San Diego, CA, as a Consultant Engineer. In July 2007, he joined the Missouri University of Science and Technology (formerly University of Missouri-Rolla), and is currently an Associate Professor with the Missouri S&T EMC Laboratory. His research interests include signal integrity and EMI designs in high-speed digital systems, dc power-bus modeling, intra-system EMI and RF interference, PCB noise reduction, differential signaling, and cable/connector designs. Dr. Fan served as the Chair of the IEEE EMC Society TC-9 Computational Electromagnetics Committee from 2006 to 2008, and was a Distinguished Lecturer of the IEEE EMC Society in 2007 and 2008. He currently serves as the Vice Chair of the Technical Advisory Committee of the IEEE EMC Society, and is an associate editor for the IEEE Transactions on Electromagnetic Compatibility and EMC Magazine. Dr. Fan received an IEEE EMC Society Technical Achievement Award in August 2009, and various Best Paper Awards from several international conferences. Dr. Jun Fan is a Fellow of the IEEE.

Introduction

With the recent progress in Internet of Things (IoT), several consumer electronic devices around the world are now connected to the Internet. These devices range from a refrigerator to a small car key fob, which is connected wirelessly to the internet access point through Wi-Fi. Although wireless technology in IoT devices provides great convenience, it also brings a lot of design challenges to RF integration engineers. As the complexity of digital subsystem increases, potential noise sources in devices such as microcontroller unit (MCU), System On Chip (SoC), high-speed traces, flexible cables, and power converters couples to a co-located wireless antenna. This unintended electromagnetic noise, called RF interference (or simply RFI) interferes the functionality of wireless radio and reduces the usable wireless range of the device.

There are a few conventional ways to mitigate RFI. For example, designers use shield can and grounding schemes to suppress noise radiation by modifying the coupling path. However, in small form-factor products, it is difficult to use a shield can due to mechanical (product design) fabrication and cost limitations. Another approach is to modify the noise source itself. Clock or slew rate can be lowered to reduce the power spectral density (PSD) of noise source in the frequency where RFI issues occur. However, modifying signal quality may reduce the signal integrity margin. A third approach is to route high-speed signals in a stripline fashion, instead of a microstrip. A stripline structure can provide better shielding compared to a microstrip structure. However, the choice of using a stripline routing or a microstrip routing can increase the PCB layer count, affect signal integrity, and also add complexity to the overall board layout. Therefore, it is important to explore alternate ways to mitigate RFI without compromising signal integrity or adding cost to the product.

Recently, fast and efficient methods to predict RFI in a real product have been introduced in [1] and [2]. Reciprocity theorem is used to estimate RFI by decomposing the overall problem into two steps - forward problem and reverse problem. In the forward problem, the noise source's near-field radiation is studied while the victim antenna is terminated. The forward problem can reconstruct noise source into an equivalent dipole moment model. In the reverse problem, the antenna is excited and the noise source is turned off. Using the equivalent dipole moment and the reverse field, RFI from noise source to antenna can be obtained. However, there has been little effort to conduct a systematic way to mitigate RFI.

In this paper, a popular consumer electronic device is studied. This small form-factor device has many complex digital sub-systems, including CPU, DDR memory, power supply, and two Wi-Fi antennas (for MIMO functionality) as shown in Fig. 1. Through measurements, it is determined that high speed DDR3 traces on the main logic board is the dominant noise source for RFI issue on the Wi-Fi antennas. Having identified the noise, the below outlined steps are followed to measure, reconstruct, and mitigate RFI issue.

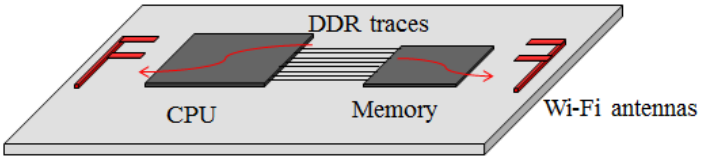

Fig. 1. DUT illustration. (could add more description here)

First, near-field measurements of source and antenna are performed using electromagnetic (EM) scanner to understand the RFI radiation and coupling physics. Then, dipole moment based reciprocity method is utilized to propose RFI mitigation methods like movement and/or rotation of noise source. The theoretical derivations and steps to maximize RFI reductions for two antennas are also provided. Finally, the results of the final modified board with reduced RFI are presented. Comparisons of measured RFI reduction and theoretical RFI reduction for both antennas are also presented.

Noise Source and Antenna Characterization

EM scanner with spectrum analyzer is a fast and convenient tool to measure near-field emissions from any radiating source. Using EM scanner, the near field distribution of noise sources (i.e., SoC and DDR3 interface) is measured. The measurement setup and a simple illustration are shown in Fig. 2. During the measurement, the device was configured in stress mode to emulate high-speed data transfer between CPU and DDR3. The resonant-type H field probe at 2.45 GHz is used and scanning is done at channel 6 of Wi-Fi. The resolution band width (RBW) of spectrum analyzer is set to 100 KHz with a sweep time of 50 ms. Average detector is used, and scan data is sampled using a max hold mode for 15 seconds. Further scanning area was chosen to be 30 mm × 30 mm with a 2 mm step.

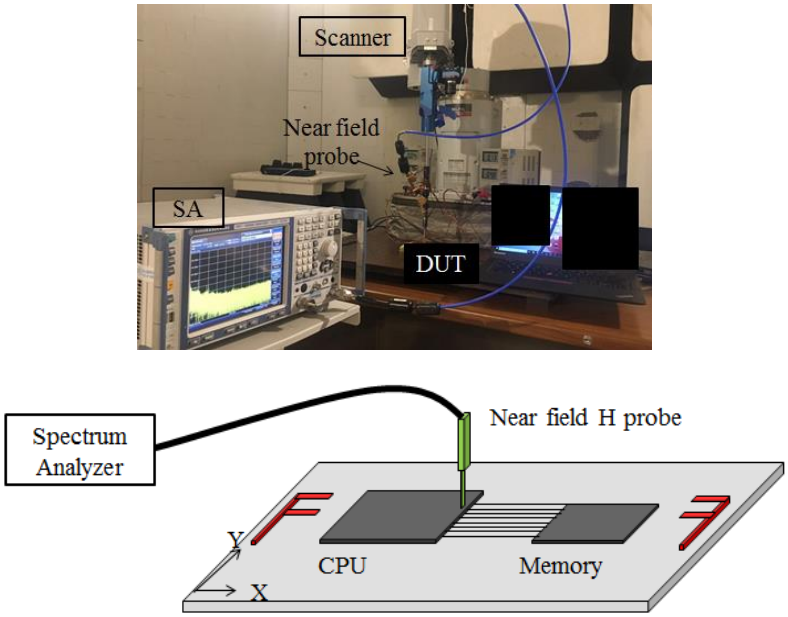

Fig. 2. A photo of the measurement set-up with a simple illustration.

The measured near-field patterns with H_x and H_y components are shown in Fig. 3(a). The H field patterns are similar to the field patterns of a single magnetic dipole M_y. Similar patterns were observed in a cell phone [3]. Once the source dipole is identified, the magnitude of the single magnetic dipole can be calculated using the least squares method with magnitude-only data [3]. Fig. 3(b) shows the near-field patterns calculated from the reconstructed magnetic dipole. According to electromagnetics theory and analysis in [3], the pattern center is the location of the dipole moment. In the measured field patterns, the pattern center corresponds to the center of the microstrip lines as depicted in Fig. 4. The reconstructed magnetic dipole M_y can be understood as an electric current loop in xz-plane facing y direction.

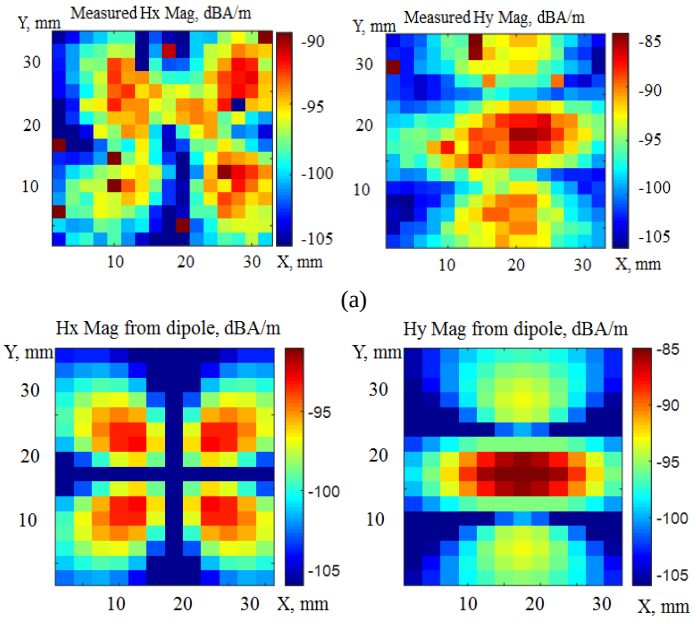

Fig. 3. (a) Measured $|H_x|$ and $|H_y|$ (b) calculated $|H_x|$ and $|H_y|$ from the reconstructed magnetic dipole.

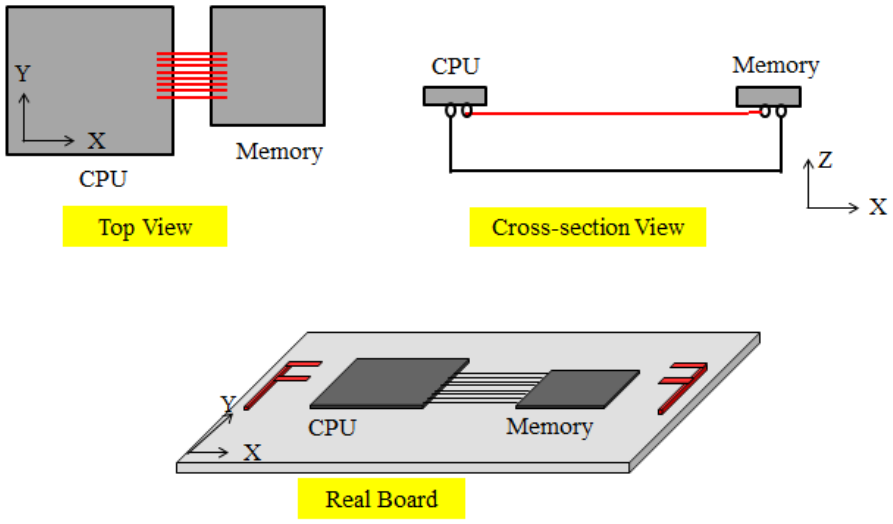

Fig. 4. Routing between the CPU and memory IC.

Since the radiation source is a single M_y dipole moment in the forward problem, according to [4], the coupled voltage to the victim antenna can be calculated by the following equation;

$$U_{fwd} = \frac{Z_L}{2U_{rev}^{+}}\left[\vec{H}_{rev} \cdot \vec{M}_{fwd}\right] \quad (1)$$

where U_{fwd} is the coupled voltage at antenna port due to the noise source, M_{fwd} is the dipole moment in the forward problem (M_y in this device), Z_L is the load impedance (50 Ω), U_{rev}^{+} is the incident voltage from the antenna port in the reverse problem, H_{rev} is the H field in the reverse problem with incident voltage of U_{rev}^{+}.

The measurement set-up of the reverse problem is shown in Fig. 5. Vector network analyzer (VNA) is used along with EM scanner instead of spectrum analyzer. The victim antenna is excited using port 1, and port 2 is connected to the near-field probe of the EM scanner. With the noise source turned off, the near-field components of antenna are measured by capturing S_{21} from VNA. Using probe calibration factor (A/m/V), S_{21} (dB) is converted to H-field (dBA/m). The measured $|H_y|$ in the reverse problem is shown in Fig. 6. In the scanning plane, it is observed there are hot spots and cold spots of antenna H-field. According to (1), smaller H_y can lead to smaller coupled voltage on the antenna port. Thus moving M_y dipole (the noise source) to the smallest H_y location can help in reducing RFI. However in this device, smallest H_y location is at the edge of the scanning plane, which is also the edge of the main logic board. If this change was applied, then CPU and memory ICs must be placed at the edge of board, which is not a practical layout change. While reducing the magnitude of forward M_y will yield similar results, the method to reduce the magnitude will lead to signal integrity issues discussed previously.

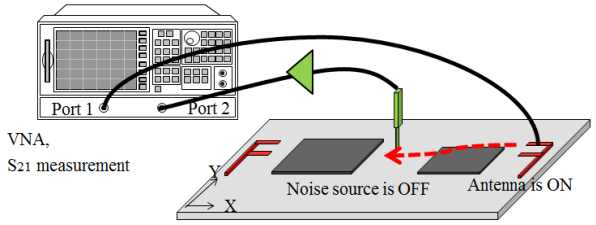

Fig. 5. Measurement setup of the reverse problem with antenna excited

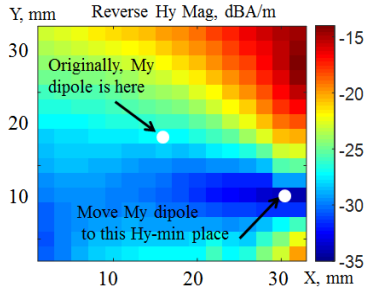

Fig. 6. Measured $|H_y|$ in the reverse problem. Moving the M_y dipole to the smallest H_y place reduces the noise coupling and alleviates RF desense issue.

RFI Reduction by Rotating Noise Source

In (1), it is worth noting that there is an inner product between two vectors: the noise source and reverse field ($\vec{H}_{rev}$ and $\vec{M}_{fwd}$). In this work, a novel method in manipulating the angle difference of two vectors is undertaken. With a certain angle, the inner product of these two vectors can be minimized. A general expression of $\vec{H}_{rev}$ and $\vec{M}_{fwd}$ is given as below:

$$\begin{aligned}\vec{H}_{rev} &= \hat{x}\,|H_x|e^{i\theta_x} + \hat{y}\,|H_y|e^{i\theta_y} + \hat{z}\,|H_z|e^{i\theta_z} \\ \vec{M}_{fwd} &= \hat{x}\,|M|e^{i\theta_m}\cos\varphi + \hat{y}\,|M|e^{i\theta_m}\sin\varphi\end{aligned} \tag{2}$$

where $\hat{x}$, $\hat{y}$, and $\hat{z}$ are the unit vectors along x-, y- and z-axes, respectively. $|H|$ and θ are the magnitude and phase of reverse H, respectively. $|M|$ and θ_m are the magnitude and phase of the original M dipole, respectively. φ is the rotation angle, relative to x-axis. Fig. 7 shows a simple diagram of the rotation problem.

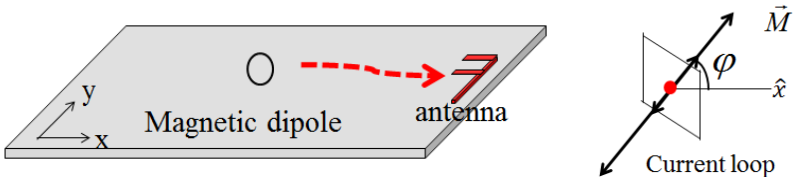

Fig. 7. Simple diagram of the rotation problem.

Substituting (2) into (1) and assuming U_{rev}^{+}=1 V, and Z_L=50 Ω, the coupled voltage can be obtained as below

$$\begin{aligned}U_{fwd} &= 25\vec{H}_{rev}\cdot\vec{M}_{fwd} = 25(\hat{x}\,|H_x|e^{i\theta_x} + \hat{y}\,|H_y|e^{i\theta_y} + \hat{z}\,|H_z|e^{i\theta_z})\cdot(\hat{x}\,|M|e^{i\theta_m}\cos\varphi + \hat{y}\,|M|e^{i\theta_m}\sin\varphi) \\ |U_{fwd}| &= 25|M|\sqrt{(|H_x|^2\cos^2\varphi + |H_y|^2\sin^2\varphi + 2|H_x||H_y|\sin\varphi\cos\varphi(\cos\theta_x\cos\theta_y + \sin\theta_x\sin\theta_y)} \\ |U_{fwd}| &= 25|M_\varphi||H_\varphi| \\ |H_\varphi| &= \sqrt{(|H_x|^2\cos^2\varphi + |H_y|^2\sin^2\varphi + 2|H_x||H_y|\sin\varphi\cos\varphi(\cos\theta_x\cos\theta_y + \sin\theta_x\sin\theta_y)}\end{aligned} \tag{3}$$

where $|M_\varphi|$ is the magnitude of the magnetic dipole after rotation angle φ in xy-plane; $|M_\varphi|$ remains the same for any rotation angle φ in xy-plane. A special case for this rotation problem is that the reverse H field is linearly polarized. Namely, the phase difference between reverse H_x and H_y fulfills the relationship such that $\theta_x - \theta_y = \pm n\pi$. Then it leads to $\cos\theta_x\cos\theta_y + \sin\theta_x\sin\theta_y = \pm 1$. In this special case, (3) is simplified as

$$\begin{aligned}|U_{fwd}| &= 25|M|(|H_x|\cos\varphi \pm |H_y|\sin\varphi) \\ |U_{fwd}| &= 25|M_\varphi||H_\varphi| \\ H_\varphi &= (|H_x|\cos\varphi \pm |H_y|\sin\varphi) \\ &= (\hat{x}\,|H_x| \pm \hat{y}\,|H_y|)\cdot(\hat{x}\cos\varphi + \hat{y}\sin\varphi)\end{aligned} \tag{4}$$

In (4), H_φ is actually an inner product of two vectors, both of which are real numbers. In contrast, (1) is also an inner product of two vectors, both of which, however, are

complex numbers. Eq (1) depicts a general case ($\theta_x - \theta_y \neq \pm n\pi$), while (4) shows the special case ($\theta_x - \theta_y = \pm n\pi$). A simple diagram is drawn in Fig. 8 to illustrate the special case ($\theta_x - \theta_y = \pm n\pi$). In Fig. 8, when the loop is placed along the reverse H field line, there are no H field lines penetrating through the current loop. Thus, the inner product between the H field vector and the normal vector of the loop is zero and no noise coupling occurs. The worst RFI for the linearly polarized case happens when the H field vector is perpendicular to the current loop. Another diagram is drawn in Fig. 9 to illustrate the general case ($\theta_x - \theta_y \neq \pm n\pi$). In Fig. 9, when the loop is placed along the longer axis of the ellipse, there are less H field lines penetrating through the current loop. Thus, the inner product between the H field vector and the normal vector of the loop becomes the minimum. The worst RFI for the elliptically polarized case happens when the H field vector is placed along the shorter axis. There are more H field lines penetrating through the current loop. Thus, the inner product between the H field vector and the normal direction of the loop becomes the maximum.

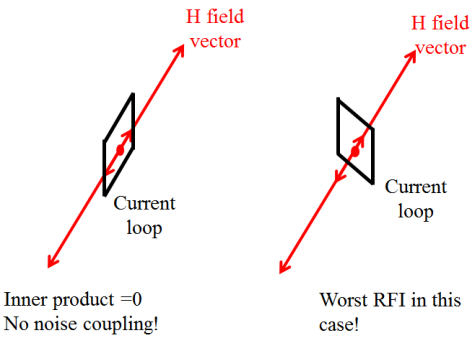

Fig. 8. A special case for the rotation problem: Reverse H field is linearly polarized ($\theta_x - \theta_y = \pm n\pi$).

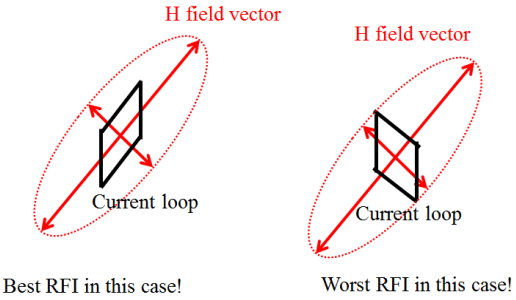

Fig. 9. A general case for the rotation problem: Reverse H field is elliptically polarized ($\theta_x - \theta_y \neq \pm n\pi$).

Taking one of the Wi-Fi antenna on this board for analysis, the magnitude and phase of reverse H_x and H_y is obtained from the reserve problem measurement. The measured phase difference of reverse H_x and H_y is 181˚, which is very close to the special case in Fig. 8 of that of a linearly polarized reverse H field. It is expected that RFI will be minimum at a certain rotation angle. By substituting magnitude and phase of reverse H_x and H_y into (3), coupled voltage at any rotation angle φ is obtained. The theoretical RFI reduction is defined by subtracting the coupled voltage at any rotation angle φ from the original coupled voltage where dipole moment is M_y (where φ is 90˚).

As stated above $|M_\varphi|$ stays the same for any rotation angle φ in xy-plane. The RFI reduction is from the reduction in $|H_\varphi|$ compared to original H_y (namely φ=90˚). Measurement is also done to show the reduction in $|H_\varphi|$ using the setup shown in Fig. 5. The baseline was set as measured $|H_y|$ when the probe is facing y direction. For any other rotation angle φ, the probe will be rotated to measure $|H_\varphi|$. The measured reduction in $|H_\varphi|$ is defined by subtracting the $|H_\varphi|$ at any rotation angle φ from the original $|H_y|$.

Measured and theoretical RFI reduction for any rotation angle φ is shown in Fig. 10. A good agreement seen between measurement and theory validates the proposed methodology. When the rotation angle is 27˚, maximum RFI reduction is achieved to be 38.8 dB. In simulation, the RFI between the original case and the φ =27˚ rotation case are compared. Simulation results are shown in Fig. 11. Simulated RFI reduction is 38 dB, which agrees with the measured and theoretical RFI reduction very well.

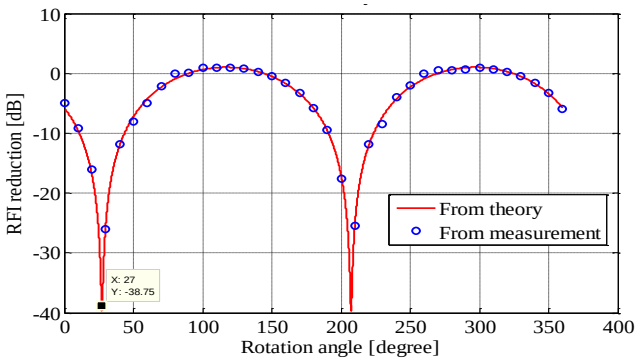

Fig. 10. Theoretical RFI reduction for various rotation angle φ. Noise source is kept at same place.

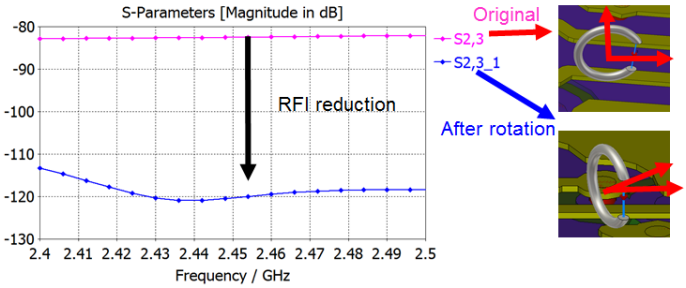

Fig. 11. RFI reduction in simulation between φ=90˚ (original case) and φ=27˚ (best rotation angle).

RFI Reduction for Two Antennas

In the previous sections, a theoretical way to improve RFI without impacting signal integrity and adding cost to the product is introduced. Simulations and measurements show that rotating the magnetic dipole moment, which is the noise source, to φ=27˚ can significantly reduce RFI for one of the selected Wi-Fi antenna on this device. However, in an actual device, the two antennas (for MIMO functionality) need to be improved together. Two special cases are studied for the two-antenna system. The first special case is that the two antennas are symmetrical around the y-axis. The second special case is that the two antennas are symmetrical to source point of magnetic dipole moment. Let us assume that the near field is a general case, i.e. elliptically polarized. Then, for the y-

symmetry case in Fig. 12(a), the best angles for RFI reduction are achieved at different angles, as denoted by the two different shorter axes of the two ellipses. In other words, there is no best angle to achieve maximum RFI reduction for both antennas. In contrast, for the point symmetry case in Fig. 12(b), the best angles for RFI reduction on both antennas is achieved along the same line, as denoted by the shorter axes of the same ellipse. For the first special case in Fig. 12(a), where two antennas are symmetrical around the y-axis, the theoretical RFI reduction can be calculated by taking the simulated magnitude and phase of H_x and H_y of both antennas into (3). The theoretical RFI reductions for both antennas are shown in Fig. 13(a). The best angle to achieve maximum RFI reduction for right-side antenna and left-side antenna is φ=27˚ and φ=153˚, respectively. In this y-symmetry case, there is no best angle to achieve maximum RFI reduction for both antennas. On the contrary, for the point-symmetry case, there is a best angle φ=27˚ to achieve maximum RFI reduction for both antennas, as shown in Fig. 13(b).

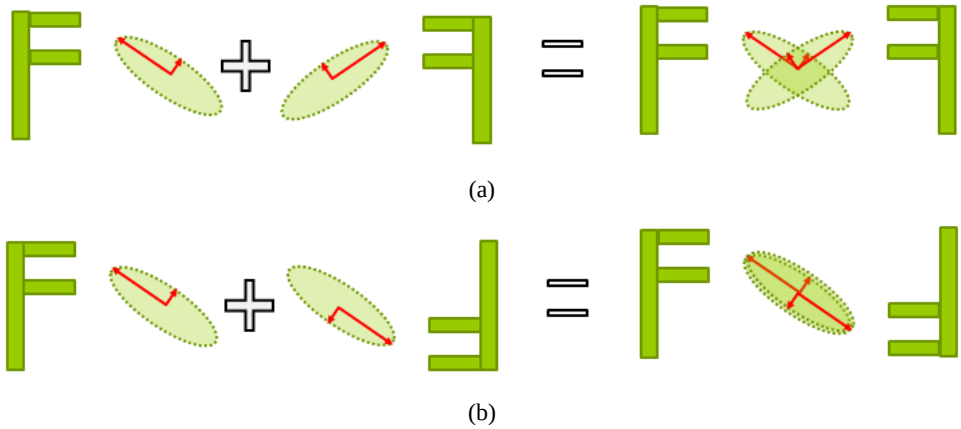

(a)

(b)

Fig. 12. RFI reduction diagram for two antennas; (a) Both antennas are symmetrical over y-axis (b) Both antennas are symmetrical over the dipole moment source point.

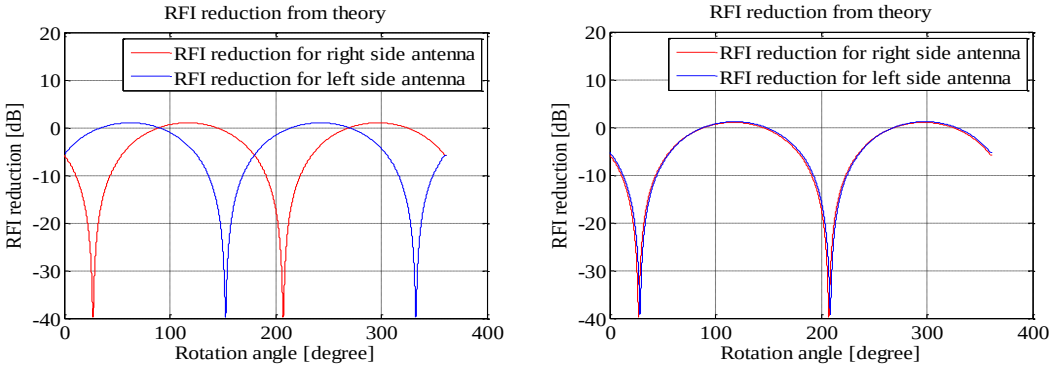

(a) (b)

Fig. 13. Theoretical RFI reduction at any rotation angle φ for two antennas: (a) both antennas are symmetrical over Y axis; (b) Both antennas are symmetrical over the dipole moment source point.

However, due to the limitation of the layout space on this board, it was difficult to rotate the dipole moment to φ=27˚ while keeping the dipole location the same and keeping two antenna point symmetrical over the dipole moment source. So the ideal case in Fig. 13 was not feasible in the real board design. In the final modified layout, the locations of the noise source were moved up 3 mm in order to accommodate the

placement of other components. Fig. 14 shows the comparisons between the original board and the final modification board. Based on the simulated reverse-field distribution of two antennas, the theoretical RFI reduction for any rotation angle φ is shown in Fig. 15. When the rotation angle φ is 27˚, the theoretical RFI reduction for the left and right side antennas are 6.5 dB and 9 dB.

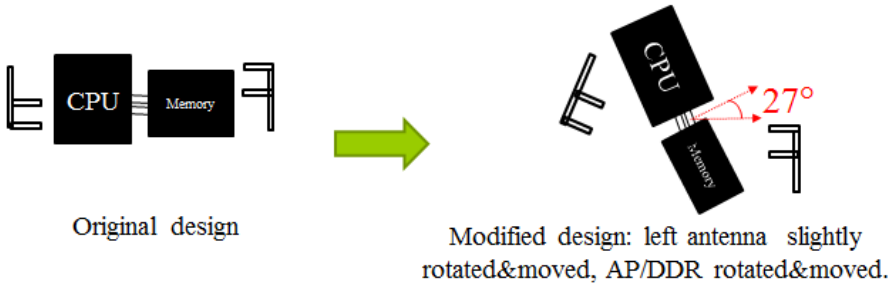

Fig. 14. The original design and the modified design.

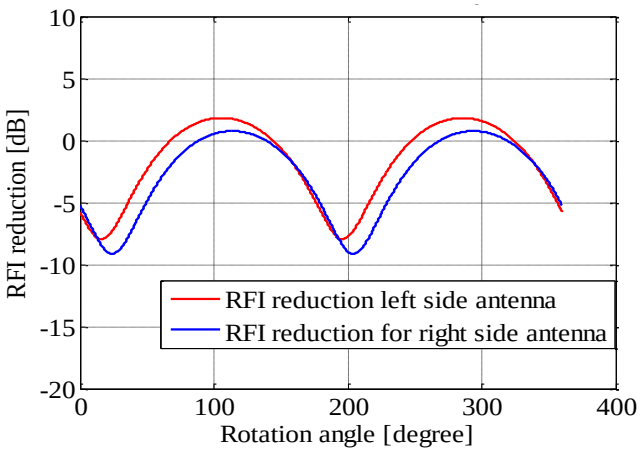

Fig. 15. The theoretical RFI reduction at any rotation angle φ for the two antennas on the modified board.

The device with the new placement has been fabricated and measured. The measured RFI for the right-side antenna between the modified design and the original design is shown in Fig. 16. The measured RFI reduction for the right-side antenna is 8 dB and for the left-side antenna is 4 dB at 2.437 GHz (channel 6 of 2.4 GHz Wi-Fi). The RFI reduction for both antennas agree well with the theoretical RFI reduction. The error is within 2.5 dB. Overall, good RFI reduction is achieved for both antennas. The proposed RFI reduction methodology is validated successfully.

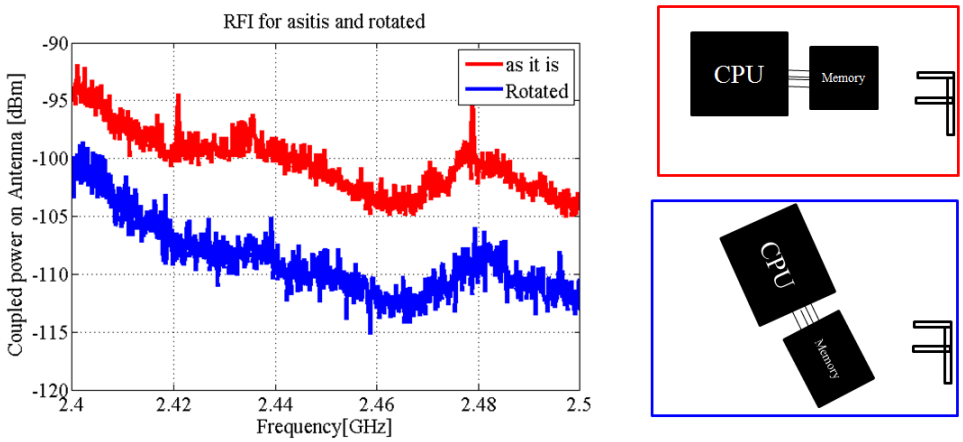

Fig. 16. Measured RFI reduction for the right-side antenna between the modified design and the original design.

Summary

RFI reduction for a real consumer electronic device is studied. Considering the layout limitation of the product, the proposed RFI mitigation involves rotating the CPU and DDR chip by a certain angle without compromising signal integrity. In addition to retaining signal integrity, the proposed method doesn't require shield can to meet RFI specification for achieving the desired Wi-Fi performance. New boards with the suggested changes were manufactured, and measured results showed a good RFI reduction (up to 8 dB) compared to the original board. The measured RFI reduction has a good agreement with theoretical RFI reduction. The proposed method enables a new dimension to RFI mitigation with cost-saving opportunities.

Acknowledgment

This work was partially supported by the National Science Foundation under Grant IIP-1440110.

Reference

[1] Y. Wang et al., "A Simulation-Based Coupling Path Characterization to Facilitate Desense Design and Debugging," in Proc. of IEEE Symp. Electromagn.Compat., 2018, pp. 150-155.

[2] Q. Huang et al., "Desense Prediction and Mitigation from DDR Noise Source," in Proc. of IEEE Symp. Electromagn.Compat., 2018, pp. 139-144.

[3] Q. Huang, F. Zhang, T. Enomoto, J. Maeshima, K. Araki and C. Hwang, "Physics-based dipole moment source reconstruction for RFI on a practical cellphone", IEEE Trans. Electromagn. Compat., vol. 59, no. 6, pp. 1693-1700, Dec. 2017.

[4] Qiaolei Huang, Takashi Enomoto, Shingo Seto, Kenji Araki, Jun Fan, Chulsoon, Hwang "Accurate and Fast RFI Prediction Based on Dipole Moment Sources and Reciprocity" in Proc. of DesignCon, 2018.